

Fig. 3.7 Case (P+I): Measurements and model simulations for initial guess and final Gauss-Newton iterate. *Left (a)*: Prey population $N_1(t)$. *Right (b)*: Predator population $N_2(t)$

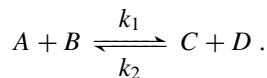
full rank 6. The final iterate came out as

$$\begin{aligned} p^* &= (\alpha^*, \beta^*, \gamma^*, \delta^*, N_1(0)^*, N_2(0)^*) \\ &= (0.481599, 0.024847, 0.925125, 0.027508, 34.910103, 3.868005) . \end{aligned}$$

The finally achieved accuracy is $3.01 \cdot 10^{-4}$, indicating that the parameter values have been determined up to 4 decimal digits. The incompatibility factor came out as $\kappa = 0.13$, for the final iterate the subcondition turned out to be $\text{sc}(F'(p^*)) = 400.0$, which here, too, confirms that the solution is unique. In fact, by leaving $N_1(0)$ and $N_2(0)$ open, a better fit than in case (P) is achieved. The least-squares functional was further reduced from $\|F(p^*)\| = 4.24$ in case (P) to $\|F(p^*)\| = 3.76$ in case (P+I). In the absence of any modelling error, this would point to a measurement error in the values $N_{1,2}(0)$, with $N_1(0) = 34.9$ thousands and $N_2(0) = 3.9$ thousands probably being the “true” values. However, model (1.10) represents a strong simplification. Certain mechanisms are missing, which is the main reason for the mismatch between data and simulation results. Nevertheless, the overall dynamical interactions between hares and lynxes are captured quite nicely by the model, as illustrated in Fig. 3.7.

3.5.2 A Simple Rank-Deficient Problem

Here we want to illustrate the importance of possible rank-deficiency in the course of the above presented Gauss-Newton iteration. For this purpose, we revisit the *bimolecular reaction* from Sect. 1.2.1, which reads



The corresponding ODE system (1.13) has been shown to be

$$A' = B' = -k_1AB + k_2CD, \quad C' = D' = +k_1AB - k_2CD,$$

wherein the rate coefficients k_1, k_2 have the role of the two parameters p_1, p_2 to be identified from a comparison with measurements. For initial values and rate coefficients we set

$$A(0) = 2, B(0) = 1, C(0) = 0.5, D(0) = 0, \quad k_1 = 0.1, k_2 = 0.2.$$

From (1.15) we recall that in the chemical *equilibrium* phase classical *mass action kinetics* holds, which can be described by a *single* parameter, the Arrhenius coefficient

$$k_{21} = \frac{k_2}{k_1} = 2.0. \quad (3.61)$$

With this insight in mind, we choose two different sets of measurements:

- *Case (T+E)*: measurement data cover both transient and equilibrium phase.
- *Case (E)*: measurement data cover equilibrium phase only.

In order to generate “measurements”, we integrate the above ODE system by means of the explicit Runge-Kutta integrator DOPRI5 (see Sect. 2.2.1) with relative and absolute accuracies $RTOL = 10^{-8}$, $ATOL = 10^{-6}$ and interpret the values computed for the adaptive time points as measurement data. In both cases, we choose the initial guesses

$$(k_1^0, k_2^0) = (0.2, 0.5)$$

to start the Gauss-Newton iteration. The required relative final accuracy of the iteration has been set to $PTOL = 10^{-4}$.

Case (T+E)

As documented in Table 3.6, the solution of the corresponding nonlinear least squares problem is obtained within 5 Gauss-Newton iterations, all of them with *full rank* 2. The final iterate came out as

$$p^* = (k_1^*, k_2^*) = (0.10000001, 0.19999997) \Rightarrow k_{21}^* = 1.9999994.$$

Obviously, this recovers the original kinetic parameter values to 7 decimal digits in agreement with the output value of the final achieved accuracy $1.8 \cdot 10^{-7}$. In passing we note the (rounded) results for the incompatibility factor $\kappa = 0.008$ and for the subcondition number $sc(F'(p^*)) = 6.3$ for the final iterate, which confirms

Table 3.6 Case (T+E): Iteration history for global Gauss-Newton method

k	$\ F(p^k)\ $	$\ \Delta p^k\ $	λ_k	Rank
0	4.81e-02	3.55e-01		2
1	2.55e-02	1.75e-01	0.389	2
2	1.04e-02	4.22e-02	1.000	2
3	9.16e-04	1.90e-03	1.000	2
4	8.00e-06	1.99e-05	1.000	2
5	3.21e-07	1.54e-09	1.000	2

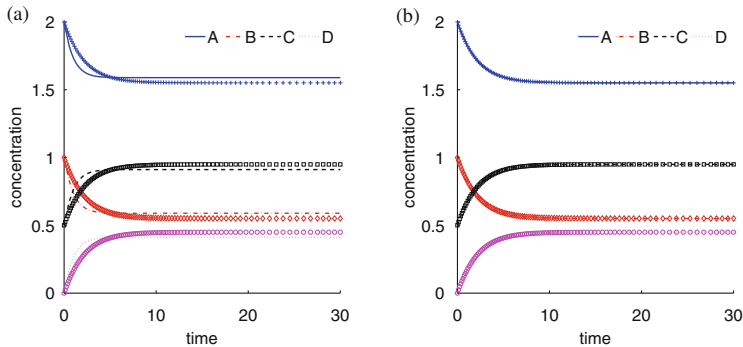


Fig. 3.8 Case (T+E): Comparison of measurements and model. *Left (a)*: Model simulation for initial guess (k_1^0, k_2^0) . *Right (b)*: Model simulation for final parameter (k_1^*, k_2^*)

Table 3.7 Case (E): Iteration history for local Gauss-Newton method (within global GN algorithm). Due to the occurrence of rank-deficiency, a unique solution cannot be expected

k	$\ F(p^k)\ $	$\ \Delta p^k\ $	λ_k	Rank
0	3.85e-02	2.96e-02		1
1	2.40e-03	1.85e-03	1.000	1
2	1.11e-05	7.67e-06	1.000	1
3	6.67e-06	6.75e-11	1.000	1

the expectation of a unique solution. In Fig. 3.8, a comparison of measurements and model for both the initial guess and the final iterate is given.

Case (E)

As documented in Table 3.7, a solution of the corresponding nonlinear least squares problem is obtained within 3 local Gauss-Newton iterations, here, however, all of them with deficient *rank* 1. This means that we cannot expect to have obtained a unique solution.

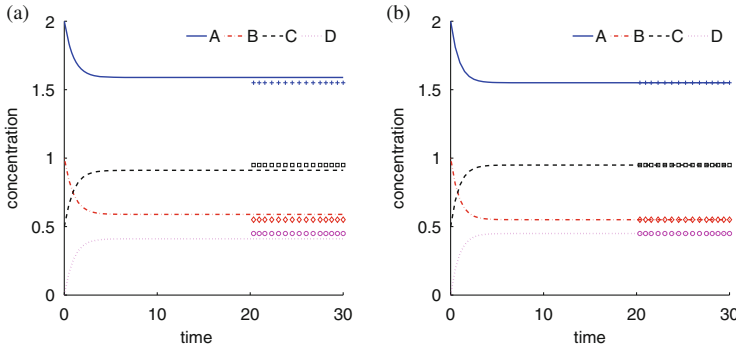


Fig. 3.9 Case (E): Comparison of measurements and model. Left (a): Simulation of model for initial guess (k_1^0, k_2^0) . Right (b): Simulation of model for final Gauss-Newton iterate (k_1^{**}, k_2^{**})

The final parameter iterate came out as

$$p^{**} = (k_1^{**}, k_2^{**}) = (0.24155702, 0.48312906) \Rightarrow k_{21}^{**} = 2.0000622.$$

Again, we note the rounded incompatibility factor (here for the rank-deficient Gauss Newton iteration) $\kappa = 0.004$. The final subcondition number (for full rank 2) came out to be $\text{sc}(F'(p^*)) = 4.5 \times 10^6$, by the way only slightly less than the condition number $\text{cond } F'(p^*) = 5.6 \times 10^6$ (computed here only for comparison reasons). In view of the numerical integration accuracy, the Jacobian accuracy value $\varepsilon_A = 10^{-4}$ has been set, compare Sect. 3.2.2. With this specification, the rule (3.18) gives rise to the observed rank deficiency. In Fig. 3.9, a comparison of measurements and model for both the initial guess and the final iterate is presented.

Clearly, the invested kinetic parameters $(k_1, k_2) = (0.1, 0.2)$ have *not* been recovered. Nevertheless, although the obtained result (k_1^{**}, k_2^{**}) is totally “off the track”, the *rank-deficient* Gauss-Newton method is able (i) to deliver a “nice fit”, see Fig. 3.9b, and (ii) to recover the Arrhenius coefficient k_{21} . The latter occurrence is in direct agreement with formula (3.30), as a careful examination would reveal (skipped here, too technical). However, it is important to understand that the obtained computational results cannot serve as interpretable values beyond the equilibrium phase.

Summary

For unaware observers it is certainly puzzling that both “solutions”, $p^* = (k_1^*, k_2^*)$ as well as $p^{**} = (k_1^{**}, k_2^{**})$, yield the same “perfectly matching” plots compared with data set (E). However, this is in agreement with the analysis given in (3.49): both solutions are minimal points in a parabolic “valley”

$$F(p) = F(p^*) + \mathcal{O}(\|p - p^*\|^2), \quad F(p) = F(p^{**}) + \mathcal{O}(\|p - p^{**}\|^2).$$

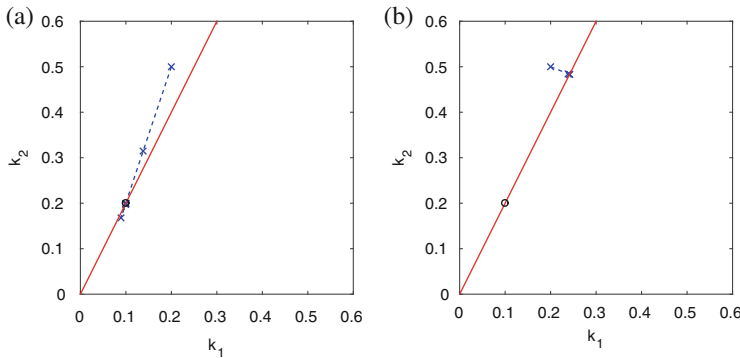


Fig. 3.10 Gauss-Newton iterations in the parameter plane. Unique solution point $p = (0.1, 0.2)$ marked as (o). Straight line represents subspace S according to (3.62). *Left (a):* Case (T+E). Full rank iteration $p^0 \rightarrow p^* = p$. Unique solution recovered. *Right (b):* Case (E). Rank deficient iteration $p^0 \rightarrow p^{**} \in S$. Observe the orthogonality of the iteration path towards the subspace

For further illustration, Fig. 3.10 shows the two cases in a (k_1, k_2) -plane. Starting from the same initial guess p^0 , both final iterates p^* and p^{**} are contained in the subset

$$S := \{(k_1, k_2) \mid k_2 - 2.0 k_1 = 0\}, \quad (3.62)$$

which was determined by the algorithm via the rank decision device within the $QR\hat{Q}$ -decomposition of the Jacobian $F'(p)$. In passing, recall that, by algorithmic construction, the Gauss-Newton corrections are orthogonal to the nullspace of the Jacobians, which, assuming not too much Jacobian variation close to the solution point p^{**} , means also roughly orthogonal to S .

Remark 13 Note that the above occurrence in the rank-deficient case is in perfect agreement with the model reduction based on chemical insight as presented in Sect. 1.2.1 above. In [35] the question of identifiability of parameters in nonlinear dynamical models has also been treated in detail. In contrast to the presently advocated techniques, that article tries to implement an *interactive* technique that does not exploit any of the information coming from the Gauss-Newton method or its local realization via some rank-deficient QR -factorization. Here, however, the model reduction has been *automatically* realized by the algorithm itself.

3.5.3 A Complex Human Menstrual Cycle Problem

In this final section, we want to present more general parameter identification techniques assumed to be helpful when treating a wider class of complex problems. For this purpose, we revisit Example 1 (Sect. 1.2.1), which models the human

A Guide to Numerical Modelling in Systems Biology

Deuflhard, P.; Röblitz, S.

2015, X, 168 p. 42 illus., 33 illus. in color., Hardcover

ISBN: 978-3-319-20058-3